Involvement of Water in Carbohydrate−Protein Binding

Christopher Clarke,[†] Robert J. Woods,*[,†] John Gluska,[†] Alan Cooper,[‡] Margaret A. Nutley,[‡] and Geert-Jan Boons*[,†]

Contribution from the Complex Carbohydrate Research Center, 220 Riverbend Road, Athens, Georgia 30602, and Department of Chemistry, University of Glasgow, Glasgow G12 8QQ, U.K.

Received December 21, 2000

Abstract: The interactions of trimannosides **1** and **2** with Con A were studied to reveal the effects of displacement of well-ordered water molecules on the thermodynamic parameters of protein−ligand complexation. Trisaccharide **2** is a derivative of **1**, in which the hydroxyl at C-2 of the central mannose unit is replaced by a hydroxyethyl moiety. Upon binding, this moiety displaces a conserved water molecule present in the Con A binding site. Structural studies by NMR spectroscopy and MD simulations showed that the two compounds have very similar solution conformational properties. MD simulations of the complexes of Con A with **1** and **2** demonstrated that the hydroxyethyl side chain of **2** can establish the same hydrogen bonds in a low energy conformation with the protein binding site as those mediated by the water molecule in the complex of **1** with Con A. Isothermal titration microcalorimetry (ITC) measurements showed that **2** has a more favorable entropy of binding compared to **1**. This term, which was expected, arises from the return of the highly ordered water molecule to bulk solution. The favorable entropy term was, however, offset by a relatively large unfavorable enthalpy term. This observation was rationalized by comparing the extent of hydrogen bond and solvation changes during binding. It is proposed that an indirect interaction through a water molecule will provide a larger number of hydrogen bonds in the complex that have higher occupancies than in bulk solution, thereby stabilizing the complex.

Introduction

Although interactions involving nucleic acids and proteins are fundamental to biology and have been well-studied, the importance of recognition processes involving carbohydrates is only recently gaining attention.[1−3] Protein−carbohydrate interactions are implicated in embryogenesis, fertilization, neuronal development, and hormonal activities, as well as in cell proliferation and organization into specific tissues. These interactions are also important in health science and are involved in the invasion and attachment of pathogens, inflammation, metastasis, blood group immunology, and xenotransplantation.[4−7] Among protein−carbohydrate complexes, those involving lectins are of considerable interest because the high specificities of these interactions has led to the use of lectins as molecular probes.[8,9]

Lectin−carbohydrate structures have been widely studied but the thermodynamics of these interactions are complex and poorly understood.[10] While counter examples exist, protein−carbohydrate associations are typified by favorable enthalpic terms that are offset by unfavorable entropic contributions. Generally, only a few hydroxyl groups of an oligosaccharide serve critical roles in determining the binding affinity and specificity. These key binding hydroxyl groups are arranged in clusters presented by different monosaccharide units.[11,12] This type of spatial grouping provides a very effective mechanism for establishing high levels of fidelity in physiological processes guided by protein−oligosaccharide recognition. Key polar groups have been identified in studies with synthetic analogues, in which hydroxyl groups were systematically replaced by either halogen or hydrogen atoms. These deoxy analogues displayed significant loss of affinity.[12−14]

Several studies have indicated that water rearrangement plays an important role in carbohydrate−protein complexation.[15−17] High-resolution protein crystal structures typically include significant areas of protein surface covered with water sites of partial occupancy, signaling either static or dynamic disorder.[18] When displaced by a saccharide ligand, this weakly bound disordered water would be expected to contribute favorably to the enthalpy of binding via return to bulk solvent where it may form stronger hydrogen bonds.

Experimental evidence that water molecules are involved in molecular association processes in aqueous solutions came from studies by Chervenak and Toone.[19] They showed that for a range

* Corresponding authors.
[†] Complex Carbohydrate Research Center.
[‡] University of Glasgow.

(1) Dwek, R. A. *Chem. Rev.* **1996**, *96*, 683−720.
(2) Gabius, H. J. *Naturwissenschaften* **2000**, *87*, 108−121.
(3) Varki, A. *Glycobiology* **1993**, *3*, 97−130.
(4) Witczak, Z. J. *Curr. Med. Chem.* **1995**, *1*, 392.
(5) Bertozzi, C. R.; Fukuda, S.; Rosen, S. D. *Biochemistry* **1995**, *34*, 14271−14278.
(6) Simanek, E. E.; McGarvey, G. J.; Jablonovski, J. A.; Wong., C. H. *Chem. Rev.* **1998**, *98*, 833−862.
(7) Gordon, E. J.; Sanders, W. J.; Kiessling, L. L. *Nature* **1998**, *392*, 30−31.
(8) Lee, Y. C.; Lee, R. T. *Acc. Chem. Res.* **1995**, *28*, 321−327.
(9) Lis, H.; Sharon, N. *Chem. Rev.* **1998**, *98*, 637−674.
(10) Toone, E. J. *Curr. Opin. Struct. Biol.* **1994**, *4*, 719−728.
(11) Lemieux, R. U. *VIIIth Int. Symp. Med. Chem.: Proc.* **1984**, *1*, 329−351.
(12) Lemieux, R. U. *Chem. Soc. Rev.* **1989**, *18*, 347−374.
(13) Oscarson, S.; Tedebark, U. *Carbohydr. Res.* **1995**, *278*, 271−287.
(14) Glaudemans, C. P. J. *Chem. Rev.* **1991**, *91*, 25−33.
(15) Lemieux, R. U.; Delbaere, L. T. J.; Beierbeck, H.; Spohr, U. *CIBA F. Symp.* **1991**, *158*, 231−248.
(16) Lemieux, R. U. *Acc. Chem. Res.* **1996**, *29*, 373−380.
(17) Ladbury, J. E. *Chem. Biol.* **1996**, *3*, 973−980.
(18) Saenger, W. *Annu. Rev. Biophys. Chem.* **1987**, *16*, 93−114.
(19) Chervenak, M. C.; Toone, E. J. *J. Am. Chem. Soc.* **1994**, *116*, 10533−10539.

10.1021/ja004315q CCC: $20.00
Published on Web 11/10/2001

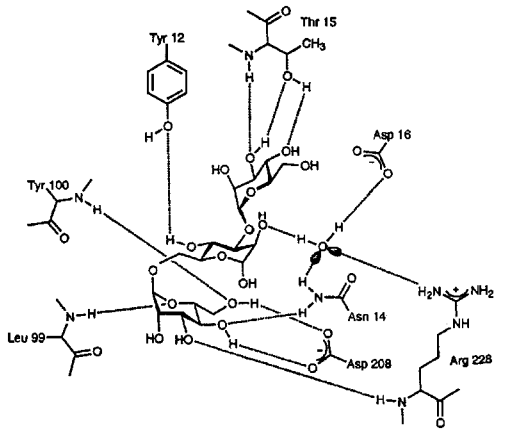

Figure 1. Hydrogen bonds between trimannoside **1** and Con A.[25]

of proteins the amount of heat liberated on binding of saccharide ligands was significantly reduced when D_2O was used as the solvent. Analysis of the isothermal microcalorimetric data indicated that 25−100% of the observed enthalpies of binding arose from dynamic reorganization of water molecules. Brewer and co-workers elegantly complemented these studies by comparing the thermodynamic date of complexation of the lectins concanavalin A (Con A) and *Dioclea grandiflora* lectin (DGL) with monodeoxy analogues of a branched trimannoside in H_2O and D_2O.[20,21] The X-ray crystal structure of DGL complexed with the trimannoside is similar to that of the Con A−trimannoside complex. The only difference exists in the location of two protein loops outside of the respective binding sites containing the amino acid residues 114−125 and 222−227. The latter residues affect the location of a network of hydrogen-bonded water molecules in the binding site of the two lectins. The measured solvent isotope effects provided evidence for altered solvation of the parent trimannoside complexes at sites consistent with the X-ray crystal structures of the lectin. However, no correlations were found between altered water structures in the DGL and Con A complexes with the trisaccharides and the $\Delta\Delta H$ values for binding to the deoxy analogues of the trisaccharide.

Dunitz has shown that the release of highly ordered water may generate a favorable entropy of up to 2 kcal mol^{-1} at 300 K.[22] This estimation was based on comparing standard heats of hydration for a number of anhydrous and hydrated inorganic salts. Studies of potent cyclic nonapeptide HIV protease inhibitors have provided support for this entropic effect.[23]

It is clear that the role of water in protein−ligand binding is complex and that further study is required. The legume lectin Con A, the most frequently studied of all lectins, provides a powerful model system for the study of protein−carbohydrate interactions. Two X-ray crystal structures of Con A complexed to two different trimannosides have been reported and are resolved to approximately 2.3 Å.[24,25] One structure involved a reducing trisaccharide[25] (Figure 1), whereas the second one was with the corresponding methyl glycoside[24] (compound **1**, Scheme 1). In the major binding mode of the ligands, all three-

Scheme 1

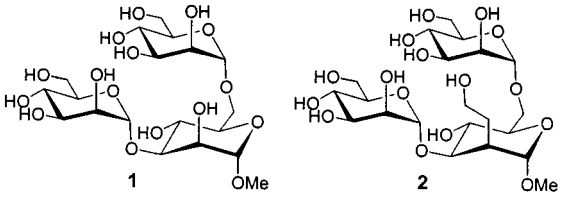

sugar units form hydrogen bonds with the protein. The α(1→6)-linked mannose residue is bound at the monosaccharide-binding site. The other two sugars are in an extended cleft. The α(1→3)-linked mannose residue, in particular, makes a strong hydrogen bond with the main chain of the protein. In addition, a highly conserved water molecule plays an important role in anchoring the reducing sugar moiety to the protein. This water makes hydrogen bonds with the C-2 hydroxyl group of the reducing mannoside and ASN-14, ASP-16, and ARG-228. The X-ray crystal structure indicates the presence of other water molecules in the carbohydrate−protein complex and, in particular, one is hydrogen bonded to the C-2 hydroxyl of the reducing mannoside (this water molecule is not indicated in Figure 1).[25]

As part of a program to probe the importance of water rearrangement in carbohydrate−protein complexation, modified trimannoside **2** (Scheme 1) was designed and synthesized, and its interactions with Con A were studied. This compound is derived from **1** but contains a hydroxyethyl moiety at C-2 of the reducing mannoside moiety, which can displace the conserved water molecule present in Con A and Con A−trisaccharide complex. An important requirement for the evaluation of the thermodynamic data of binding of **2** is that its hydroxyethyl side chain should establish the same hydrogen bonds with the protein as those mediated by the water molecule in the complex with **1**. The hydroxyethyl side chain should make these interactions in a low-energy conformation. Furthermore, compound **2** should have similar conformational properties to those of the parent compound **1**. To confirm these requirements, the solution conformations of **1** and **2** were determined by NMR spectroscopy in combination with molecular dynamics (MD) simulations. The bound conformations of **1** and **2** were also studied by MD simulation. The thermodynamic parameters of binding of Con A with **1** and **2** were obtained by isothermal titration calorimetry (ITC) measurements at several temperatures. An interpretation of the thermodynamic parameters of protein−ligand complexation based on the displacement of highly ordered water is provided.

Results and Discussion

Conformational Analysis. The solution properties of **1** and **2** were studied by NMR spectroscopy and MD simulations. Further, MD analysis was used to assess the extent to which binding to Con A altered the internal motion of **1** and **2**, relative to the motion of the unbound ligands. Predicted hydrogen bonding networks in the complexes were compared to those present in X-ray crystal structures of the trimannoside−Con A complex.[24,25]

NOE Analysis. Resonance assignments of **1** are in good agreement with data previously reported.[26] The ^1H and ^{13}C spectra of **2** were completely assigned by a combination of COSY, TOCSY, and HSQC experiments. NMR-based distance constraints between pairs of protons are frequently employed to derive a preliminary conformational model. These constraints can be derived by using the isolated spin-pair approximation

(20) Dam, T.; Oscarson, S.; Sacchettini, J. C.; Brewer, F. C. *J. Biol. Chem.* **1998**, *273*, 32826−32832.
(21) Rozwarski, D. A.; Swami, B. M.; Brewer, F.; Sacchettini, J. C. *J. Biol. Chem.* **1998**, *273*, 32818−32825.
(22) Dunitz, J. D. *Science* **1994**, *264*, 670−670.
(23) Delucca, G. V.; Erickson-Viitanen, S.; Lam, P. Y. S. *Drug Discov. Today* **1997**, *2*, 6−18.
(24) Loris, R.; Maes, D.; Poortmans, F.; Wyns, L.; Bouckaert, J. *J. Biol. Chem.* **1996**, *271*, 30614−30618.
(25) Naismith, J. H.; Field, R. A. *J. Biol. Chem.* **1996**, *271*, 972−976.
(26) Brisson, J.-R.; Carver, J. P. *Biochemistry* **1983**, *22*, 1362−1368.

Table 1. Experimental and MD-Derived Interproton Relative NOEs (%) and Proton−Proton Distances (R_{HH}, Å) for Free Ligands **1** and **2**

		NOE		R_{HH}	
ligand	spin pair	exptl	MD	exptl[a]	MD
1					
α(1→3)	H1′−H2′	0.42	0.38		2.50 ± 0.10
	H1′−H3	0.55	0.53	2.39	2.41 ± 0.22
α(1→6)	H1″−H2″	0.49	0.38		2.50 ± 0.10
	H1″−H6-*pro-R*	ND	0.20		2.91 ± 0.39
	H1″−H6-*pro-S*	0.48	0.32	2.50	2.59 ± 0.25
2					
α(1→3)	H1′−H2′	0.43	0.38		2.50 ± 0.09
	H1′−H3	0.76	0.52	2.27	2.41 ± 0.21
α(1→6)	H1″−H2″	0.40	0.38		2.49 ± 0.10
	H1″−H6-*pro-R*	ND	0.13		2.93 ± 0.38
	H1″−H6-*pro-S*	0.64	0.32	2.30	2.60 ± 0.25

[a] Computed from the experimental NOE data using the isolated spin-pair approximation.

from relative NOE intensities. This approach assumes a simple r^{-6} distance dependence of the NOE intensity between a given pair of protons, which is valid at short mixing times where NOE buildup curves are essentially linear. Good linearity of the NOE buildup curves was observed up to a mixing time of 250 ms. The interproton distances were determined by using the intra ring H1−H2 NOE as an internal reference,[27,28] at a mixing time of 100 ms (Table 1). For compound **1**, a large interresidue NOE was observed between H1 of the α(1→3)-linked residue and H3 of the core mannosyl residue. Saturation of the H1 resonance also gave rise to small NOE to H4, which presumably arose from strong coupling effects. A single interresidue NOE was observed between H1 of the α(1→6) linked residue and the *pro-S* proton at C6 (H6S) of the 1→6 linkage.

Compound **2** showed a similar NOE pattern compared to that of **1**. In this case, the frequencies of the *pro-R* and *pro-S* protons at C6 were assigned as follows: irradiation of the anomeric proton at 4.82 ppm of the α(1→6) linked mannosyl unit produced a single interresidue NOE at 3.62 ppm, which was assigned by analogy with **1** to H6*S*. The values of the H5−H6 coupling constants were in agreement with the general trend of $^3J_{H5,H6R} > {}^3J_{H5,H6S}$ by ∼2.0 Hz, a characteristic that has been observed in all cases studied.[29] Additionally, the order of the chemical shifts of H6*R* and H6*S* was in agreement with predictions of Ohrui and co-workers[30] for α(1→6) linkages, where the proximity of the ring oxygen to H6*R*, in the *exo*-anomeric conformation, leads to deshielding and a downfield shift of H6*R* relative to H6*S*.

$^3J_{HH}$ Coupling Constants. The homonuclear vicinal coupling constants $^3J_{H5,H6R}$ and $^3J_{H5,H6S}$ were used to determine the rotamer population of the ω-dihedral angle of the α(1→6) linkage by employing a set of Karplus-type empirical equations.[31] The coupling constants, measured from the NMR experiments, for **1** were $^3J_{H5,H6R} = 4.5$ Hz and $^3J_{H5,H6S} = 1.8$ Hz, which gave rise to a ratio of *gg*:*gt*:*tg* = 0.72:0.43:−0.15. The presence of a negative *tg* population has been attributed to inaccuracies in the empirical equations and is commonly corrected by setting the *tg* population to zero.[32] Several attempts have been made to increase the accuracy of values predicted by the equations, including the adoption of nonidealized staggered conformations[30] and the inclusion of vibrations about the minima.[32] For each case, negative *tg* populations were obtained. In view of the fact that there is not a definitive solution to the problem, we have chosen to use the values based on the perfectly staggered model. Thus, upon setting the population of the *tg* rotamer to zero, a population distribution of *gg*:*gt* = 0.59:0.41 was determined, which is in good agreement with data reported by Carver et al.[26] For **2**, values of $^3J_{H5,H6R} = 3.0$ Hz and $^3J_{H5,H6S} = 1.0$ Hz were measured, which after correction for a minor negative *tg* population, gave a distribution of *gg*:*gt* = 0.79:0.21.

Table 2. Trans-Glycosidic Heteronuclear *J*-Coupling Constants (Hz) and Resultant Dihedral Angles (deg) for Free Ligands **1** and **2**

ligand	linkage	$^3J_{CH}$	NMR	MD
1				
α(1→3)				
ϕ	H1′−C1′−O1′−C3	2.8	−46 ± 6[a]	−52 ± 11
ψ	C1′−O1′−C3−H3	5.4	0 ± 15	−4.8 ± 20
α(1→6)				
ϕ	H1″−C1″−O1″−C6	2.3	−52 ± 6	−53 ± 13
ψ	C1″−O1″−C6−H6-*R*	1.7	173 ± 8[b]	180 ± 27[b]
	C1″−O1″−C6−H6-*S*	3.3		
2				
α(1→3)				
ϕ	H1′−C1′−O1′−C3	2.7	−47 ± 5	−52 ± 11
ψ	C1′−O1′−C3−H3	ND	ND	−3 ± 16
α(1→6)				
ϕ	H1″−C1″−O1″−C6	2.1	−54 ± 5	−53 ± 17
ψ	C1″−O1″−C6−H6-*R*	2.3	−172 ± 10[b]	−155 ± 41[b]
	C1″−O1″−C6−H6-*S*	2.3		

[a] Error derived by assuming 0.5 Hz error in coupling constants. [b] Reported as the value for the C1″−O1″−C6−C5 angle.

$^3J_{CH}$ Coupling Constants. Further conformational properties of the trisaccharides were obtained by measurement of vicinal *trans*-glycosidic heteronuclear coupling constants, which are sensitive to the dihedral angles of glycosidic linkages (ϕ and ψ) (Table 2).[33] For compound **2**, only $^3J_{(C1',H3)}$ could be measured and was consistent with a $\phi_{(1-3)}$ dihedral angle of −47 ± 5°. Similarly, for both **1** and **2** the value of the $\phi_{(1-6)}$ dihedral angle was determined from $^3J_{(H1'',C6)}$ to be approximately −53°. In the case of **1**, the combined values of $^3J_{(C1'',H6R)}$ and $^3J_{(C1'',H6S)}$ gave a dihedral angle of $\psi_{(1-6)} = 173 \pm 8°$, which is in good agreement with an X-ray crystal structure of a related disaccharide Man-(1→6)-Man-OMe[34] and earlier solution studies. For compound **2**, the sign of the dihedral angle was changed; however, the resulting value of $\psi = -172 \pm 10°$, was close to that of **1**.

While it would have been desirable to determine the solution conformation of the ethyl moiety in **2**, this was not feasible, as it was impossible to assign the prochirality of the relevant protons in the NMR spectra. Without the ability to distinguish between the *pro-R* and *pro-S* protons, it was not possible to convert the *J*-couplings to torsion angles. Conformational analysis of this moiety would have to rely on the MD simulations alone.

Molecular Dynamics Simulations. Unrestrained MD simulations were used to assess the extent to which binding altered the ligands dynamics and conformation. Further, using the trajectories for the glycosidic torsion angles and Haasnoot's

(27) Homans, S. W.; Dwek, R. A.; Rademacher, T. W. *Biochemistry* **1987,** *26*, 6553−6560.
(28) Homans, S. W.; Dwek, R. A.; Rademacher, T. W. *Biochemistry* **1987,** *26*, 6571−6578.
(29) Carver, J. P.; Brisson, J.-R. In *Biology of carbohydrates*; Gainsburg, V., Robbins, P. W., Eds.; Wiley: New York, 1984; pp 289−331.
(30) Nishida, Y.; Hori, H.; Ohrui, H. *J. Carbohydr. Chem.* **1988**, *7*, 239−250.
(31) Haasnoot, C. A. G.; De Leeuw, M.; Altona, C. *Tetrahedron* **1980**, *36*, 2783−2792.
(32) Bock, G.; Duus, J. O. *J. Carbohydr. Chem.* **1994**, *13*, 513−543.
(33) Tvaroska, I.; Hricovini, M.; Petrakova, E. *Carbohydr. Res.* **1989**, *189*, 359−362.
(34) Bouckaert, J.; Hamelryck, T. W.; Wyns, L.; Loris, R. *J. Biol. Chem.* **1999**, *274*, 29188−29195.

equation,[31] relating this angle to the coupling constant, average values for the homonuclear *J*-coupling constants were computed. Although it is common practice to use experimental data (for example, interproton distances or *J*-coupling values) to restrain MD simulations, this has several negative aspects. First, such an approach removes any predictive capability from the modeling. Second, distance or angular constraints can be interpreted in terms of a real structure only if it is assumed that the molecule exists in a single, well-defined conformation.[35]The existence of molecular motion around glycosidic linkages, particularly in the case of 1→6 linkages, however, is well-established,[27,36−40] and a restrained simulation will not lead to a model that includes these motions. Given a sufficiently accurate force field and simulation protocol, it is clearly preferable to avoid the use of restraints.

Molecular Dynamics of Free Ligands. MD trajectories for **1** and **2** were computed in the presence of explicit water at room temperature and atmospheric pressure, using the GLYCAM carbohydrate parameters with the AMBER force field. This modeling protocol for oligosaccharides has been shown to give accurate torsional properties for glycosidic linkages without requiring any experimental constraints.[41] Also presented in Table 2 are the average dihedral angles of the glycosidic linkages of compounds **1** and **2** extracted from a 20-ns MD simulation. The simulations indicated that the ϕ and ψ angles of the α(1→3) and α(1→6) glycosidic linkages of **1** and **2** populated single conformational states whose average values were in close agreement with those determined from heteronuclear trans glycosidic coupling constant measurements.[26] The predicted ϕ and ψ angles in **1** agree well with previously reported solution conformations determined by NOE measurements, as well as from HSEA and semiempirical calculations.[42] Additionally, an X-ray crystal structure of the related trisaccharide Man-α-(1→3)-Man-*β*-(1→4)-GlcNac showed values of $\phi = -58°$ and $\psi = -19°$ for the α(1→3) linkage, which compare favorably with the MD-derived values.[43]

The 1→6 linkage differs from other glycosidic linkages in that it contains an additional rotatable bond, which may be characterized by the $O_6-C_6-C_5-O_5$ torsion angle (ω-angle). While three stable staggered rotamers are possible for the ω-angle [gauche−trans (*gt*), trans−gauche (*tg*), and gauche−gauche (*gg*), referring to the orientations of the ω-angle and the $O_6-C_6-C_5-C_4$ angle, respectively (Scheme 1)], the conformational families about the C_5-C_6 bond display a bias for gauche orientations. In contrast to the single rotamers seen for the ϕ and ψ angles, the ω−angle in both **1** and **2** displayed transitions between the *gt* and *gg* conformations. The trajectories indicated a gg:gt rotamer ratio of approximately 0.70:0.30 with less than 1% *tg* present, for both **1** and **2** (Figure 2). These results are in excellent agreement with the NMR data. The fact that the populations correctly indicate the preference of the *gg* rotamer is encouraging, particularly given the traditionally poor

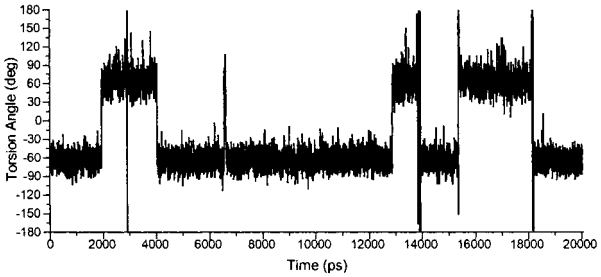

Figure 2. MD trajectory for the O6−C6−C5−O5 ω angle in **1**.

performance of MD simulations of 1→6-linked carbohydrates. Factors affecting the ability of classical force fields to model 1→6 linkages have been recently discussed.[44] The fact that the MD data do not reproduce the slight difference in ω-angle populations, between **1** and **2**, as suggested by the NMR data, may be due to the short real-time scale of the MD simulations. To our knowledge the simulations performed here are an order of magnitude longer than any reported study to date for a solvated 1→6-linked carbohydrate. The trajectories, however, exhibited only three to four transitions between the *gg* and *gt* rotamers. Much longer trajectories may still be necessary in order to achieve an accurate statistical distribution of the ω-angle populations.

Theoretical $^3J_{HH}$ Coupling Constants. Having an accurate MD trajectory for the 1→6 linkage offered the possibility to compute average values for $^3J_{HH}$ coupling constants and compare these directly with the experimental values. This approach avoided the need to make assumptions about the rotamer populations. Applying the Haasnoot equation[31] our trajectory for **1** resulted in $^3J_{H5,H6R} = 4.8$ Hz and $^3J_{H5,H6S} = 3.5$ Hz. The corresponding experimental values were 4.5 and 1.8 Hz, respectively. For **2**, the computed coupling constants were essentially identical to those for **1**, whereas the corresponding experimental values were 3.0 and 1.0 Hz, respectively. While the values for $^3J_{H5,H6R}$ are in good agreement with the experimental data, the theoretical values for $^3J_{H5,H6S}$ are consistently too large. The extent to which this is due to approximations inherent in the use of an empirical Karplus-type relationship, rather than to inaccuracies in the simulation data, is unclear. A small change in rotamer population may affect the computed *J*-value considerably.

Collectively, the NMR and MD data show that in solution, compounds **1** and **2** have very similar conformational properties. Both display the same preferred conformations about the ω-angle, with the remaining glycosidic torsion angles populating single conformations that are indistinguishable between the two molecules. The conformation of the side chain of compound **2** may be described by the two dihedral angles χ_1 and χ_2. The MD simulations indicate that free in soluion, the χ_1 angle populated two of the three possible staggered conformers, whereas χ_2 populated all three (Table 3). This moiety became noticeably more rigid upon binding of **2** to Con A.

Molecular Modeling of Complexes between Con A and the Trisaccharide. MD simulation of the complex between **1** and Con A showed that the trisaccharide was present in a single conformation that was very similar to the major conformation found from X-ray diffraction[24,25] and to the solution conformation (Table 3). Notably, the ω-angle of the α(1→6) linkage remained in the *gg* conformation throughout the simulation. The conformational properties of trisaccharide **2** complexed to Con A were very similar to those of **1**. As in the case of the ω-angle,

(35) Jardetzky, O. *Biochim. Biophys. Acta* **1980**, *621*, 227−232.
(36) Carver, J. P.; Cumming, D. A. *Pure Appl. Chem.* **1987**, *59*, 1465−1476.
(37) Peters, T.; Meyer, B.; Stuike-Prill, R.; Somarjai, R.; Brisson, J. R. *Carbohydr. Res.* **1993**, *238*, 49−73.
(38) Carver, J. P. *Pure Appl. Chem.* **1993**, *65*, 763−770.
(39) Peters, T.; Pinto, B. M. *Curr. Opin. Struct. Biol.* **1996**, *6*, 710.
(40) Imberty, A.; Hardman, K. D.; Carver, J. P.; Perez, S. *Glycobiology* **1991**, *1*, 631−642.
(41) Woods, R. J.; Pathiaseril, A.; Wormald, M. R.; Edge, C. J.; Dwek, R. A. *Eur. J. Biochem.* **1998**, *258*, 372−386.
(42) Biswas, M.; Rao, V. S. R. *Int. J. Quantum Chem.* **1981**, *20*, 99−121.
(43) Warin, V.; Baert, F.; Fouret, R.; Strecker, G.; Spik, G.; Fournet, B.; Montreuil, J. *Carbohydr. Res.* **1979**, *76*, 11−22.
(44) Kirschner, K. N.; Woods, R. J. *Proc. Natl. Acad. Sci., U.S.A.* **2001**, *98*, 10541−10545.

Table 3. Dihedral Angles (deg) and Populations {%} for Bound Ligands **1** and **2** Derived from MD Simulations of Ligand−Con A Complexes

dihedral angle	ligand **1**	ligand **2**
α(1→3)		
ϕ	-50 ± 9	-56 ± 8
ψ	9 ± 17	1 ± 11
α(1→6)		
ϕ	-44 ± 10	-40 ± 10
ψ	-172 ± 9	-167 ± 8
χ_1 {bound, free}		-69 ± 14 {14, 77}
		-168 ± 13 {86, 23}
χ_2 {bound, free}		71 ± 14 {0, 23}
		-66 ± 15 {0, 12}
		180 ± 14 {100, 65}

Table 4. Comparison of Hydrogen Bond Lengths (Å) and Occupancies {%} between the Protein and Trimannosides **1** and **2**

		heavy atom separation		
donor	acceptor	MD[a]	X-ray[25]	X-ray[24]
	Reducing Mannoside			
HO4	TYR-12 OH	2.8 ± 0.2 {93}	2.8	2.8
		2.9 ± 0.2 {98}		
	α(1→3) Terminal Mannoside			
HO3	THR-15 OG1	2.9 ± 0.3 {45}	2.9	3.1
		2.9 ± 0.2 {25}		
HO4	THR-15 OG1	2.8 ± 0.2 {46}	3.1	3.4
		2.8 ± 0.1 {67}		
THR-15 HN	O3	3.4 ± 0.4 {61}	2.8	3.2
		3.2 ± 0.3 {92}		
ASP-16 HN	O4	3.2 ± 0.3 {83}		
		3.1 ± 0.3 {97}	3.0	2.8
	α(1→6) Terminal Mannoside			
HO4	ASP-208 OD1	3.4 ± 0.3 {100}	2.7	3.7
		3.0 ± 0.4 {100}		
HO4	ASP-208 OD2	2.6 ± 0.1 {96}	2.9	2.5
		2.6 ± 0.3 {52}		
HO6	ASP-208 OD1	2.7 ± 0.2 {97}	3.2	3.2
		2.9 ± 0.5 {64}		
HO6	ASP-208 OD2	3.8 ± 0.1 {56}	2.9	4.0
		3.8 ± 0.1 {25}		
ASN-14 HND2	O4	2.9 ± 0.1 {100}	2.9	3.1
		2.9 ± 0.1 {100}		
TYR-100 HN	O6	3.2 ± 0.2 {100}	3.1	2.9
		3.2 ± 0.2 {99}		
ARG-228 HN	O3	2.9 ± 0.1 {100}	2.9	2.9
		2.9 ± 0.1 {100}		
ARG-228 HN	O4	3.3 ± 0.2 {56}	3.5	3.2
		3.4 ± 0.2 {59}		

[a] Upper value refers to the complex with **1**; lower value to that with **2**.

the side chain dihedral angles χ_1 and χ_2 also displayed less flexibility. The χ_1 dihedral angle adopted two orientations that were present in solution, although the relative populations were reversed. Notably, in the complex the χ_2 dihedral angle existed in a single conformer, which was the one most populated in solution ($\chi_2 = 180°$). The change in the ratio of conformer populations was caused primarily by formation of a hydrogen bond with ASN-14.

The hydrogen bonding patterns of both complexes were examined over the course of the MD simulations. Apart form the C-2 substituent, all other hydroxyls of **1** and **2** formed essentially identical hydrogen bond networks with the protein, which were also in excellent agreement with those observed in the X-ray structures. These interactions have been discussed in detail elsewhere[24,25] and are summarized in Table 4. The possible role played by these interactions in stabilizing ligand orientation has also been noted.[24] An attractive feature of the MD analysis is the ability to unambiguously assign hydrogen bond donor and acceptor atoms. This is particularly significant in the case where the interaction is between two or more hydroxyl groups. For example, HO3 and HO4 in the terminal α(1→3)-linked mannosyl residue both interact with THR-15. From the MD data it is clear that in these interactions the sugar hydroxyl groups function as the donor moieties. This is also the case for the interaction between HO4 of the reducing mannosyl residue and TYR-12. Assignments of the donor−acceptor atoms for these interactions, postulated on the basis of X-ray data alone, appear to be incorrect.[24]

Presented also in Table 4 are hydrogen-bond occupancies derived from the MD data. This information provides insight into the dynamic nature of some of the hydrogen bonds. Again, in the case of the hydroxyl−hydroxyl interactions involving THR-15, it can be seen that HO3 and HO4 alternate as hydrogen bond donors but do not both donate a proton to THR-15 at any one time. Last, the MD data may be used to provide an indirect measure of the strength of the hydrogen bonds, not only from the internuclear distances, but also from the occupancies and standard deviations.[45] This is exemplified for the strong interaction between ARG-228 HN and O3 of the terminal α(1→6) mannosyl residue, in contrast to the corresponding weak interaction with O4.

Table 5. Hydrogen Bond Lengths (Å) Involving the Conserved Water (OW) in the Complex with **1** vs Those Involving the Side-Chain Oxygen (OS) in the Complex with **2**

ligand	H bond pair	MD	X-ray[24,a]	X-ray[25,a]
1	OW ASP-16 OD1	2.6	2.7	2.5
2	OS ASP-16 OD1	2.8		
1	OW ASP-16 OD2	3.5	3.2	2.9
2	OS ASP-16 OD2	3.1		
1	OW ASN-14 ND2	2.9	2.7	2.6
2	OS ASN-14 ND2	2.8		
1	OW ARG-228 NH2	3.7	3.2	3.3
2	OS ARG-228 NH2	3.1		
1	OW MANO2	2.8	2.6	3.2

[a] Average values for major binding mode.

Examination of the interactions of hydroxyl group HO2 of the central mannose residue of **1** with the conserved water molecule, jointly coordinated with ASN-14, ASP-16, and ARG-228, showed a stable interaction consistent with experimental data (Table 5, Figure 1). The strongest hydrogen bonds were observed between ASN-14, the water molecule, and hydroxyl group HO2, for which a strong interaction was maintained until the water molecule dispersed from the binding site after approximately 600 ps. A weaker hydrogen bond, which broke after 100 ps, was made between the water molecule and the ASP-16 residue. The hydrogen bond between ARG-228 and the conserved water molecule was broken almost immediately and was not restored. These results compared favorably with data from the X-ray crystal structure, in which the hydrogen bond with ARG-228 is weak (Table 5). On the other hand, the hydrogen bonds bridging ASN-14, the water molecule, and HO2 of the mannose residue made close contacts in the X-ray crystal structure. These interactions were maintained until the water molecule dispersed into the bulk solvent (Table 5).

The MD data indicated that the hydroxyl group of the side chain of **2** and the conserved water molecule in the complex with **1** make very similar interactions with the binding site residues (Table 5). The interaction with ASP-16 was less stable, and after 100 ps, the separation increased to the limit of a

(45) Pathiaseril, A.; Woods, R. J. *J. Am. Chem. Soc.* **2000**, *122*, 331−338.

Table 6. Thermodynamic Parameters[a] for the Interaction between Con A and Ligands **1** and **2**

ligand	T	K_a	ΔH	ΔG	ΔS
1	283.15	8.18	-11.6 ± 0.3	-7.66 ± 0.05	-13.7 ± 1.2
	298.15	3.74	-13.3 ± 0.7	-7.60 ± 0.07	-19.2 ± 2.3
	310.15	1.95	-14.5 ± 0.6	-7.50 ± 0.09	-22.5 ± 2.5
2	283.22	1.13	-9.1 ± 0.1	-6.55 ± 0.01	-9.05 ± 0.5
	291.15	0.71	-9.8 ± 0.1	-6.46 ± 0.01	-11.3 ± 0.3
	298.15	0.49	-11.0 ± 0.6	-6.40 ± 0.03	-15.5 ± 2.0
	310.15	0.26	-11.7 ± 0.4	-6.25 ± 0.02	-17.6 ± 1.5

[a] Units are K (T), M^{-1} 10^{-5} (K_a), kcal mol^{-1} (ΔH, ΔG), cal K^{-1} mol^{-1} (ΔS).

hydrogen bond. Similarly, the interaction with ARG-228 varied more widely and showed a pattern of breaking and reforming during the course of the simulation.

The presence of a structurally conserved water molecule is also seen in the X-ray crystal structure of *Lathyrus ochrus* lectin,[46,47] which differs from Con A by replacement of ASP-16 and ARG-228 with nonpolar ALA and GLY residues. The insensitivity of the water position to these mutations indicates that the ASN-14 residue is primarily responsible for ligating the water molecule. In the simulations the interactions between ASN-14 with the conserved water, or with the hydroxyl group of the side chain in **2**, were well described.

Complexation Studies. Based on the promising structural studies, the thermodynamic parameters of binding Con A with **1** and **2** were determined by ITC measurements and the results are summarized in Table 6. In all cases, the data were consistent with simple 1:1 protein−ligand complexation, with exothermic binding offset by unfavorable entropy changes. The data for **1** are in agreement with previously reported data under similar conditions.[19−21,48−50] Binding of **2** to the protein is less favorable than for **1**, with $\Delta\Delta G^\circ = \Delta G^\circ$ (**2**) $- \Delta G^\circ$ (**1**) $= +1.2$ kcal mol^{-1} and correspondingly different enthalpy and entropy contributions: $\Delta\Delta H^\circ = +2.3$ kcal mol^{-1}, $\Delta\Delta S^\circ = +4$ cal K^{-1} mol^{-1} (298 K). Both ligands show a small but significant temperature dependence in ΔH, with binding becoming more exothermic with increasing temperatures, with correspondingly negative ΔC_p:ΔC_p(**1**) $= -109$ (± 5) cal K^{-1} mol^{-1} and ΔC_p(**2**) $= -92$ (± 13) cal K^{-1} mol^{-1}, respectively.

The more favorable entropy of complexation of **2** with Con A was anticipated, since a report by Dunitz[22] indicates that the release of highly ordered water to bulk solution can generate a favorable entropy of as much as 2 kcal mol^{-1} at 300 K. In addition, X-ray data of Con A structures showed that the conserved water molecule is more ordered when a saccharide is complexed to the protein. In the lectin−carbohydrate complex the water molecule makes hydrogen bonds to ASN-14, ASP-16, and ARG-228. On the other hand, in the uncomplexed protein the water molecule makes hydrogen bonds to ASN-14 and ARG-228 only.[51] Thus, upon saccharide binding, the water molecule is further restricted in its mobility, contributing additionally to the unfavorable entropy term of complexation.

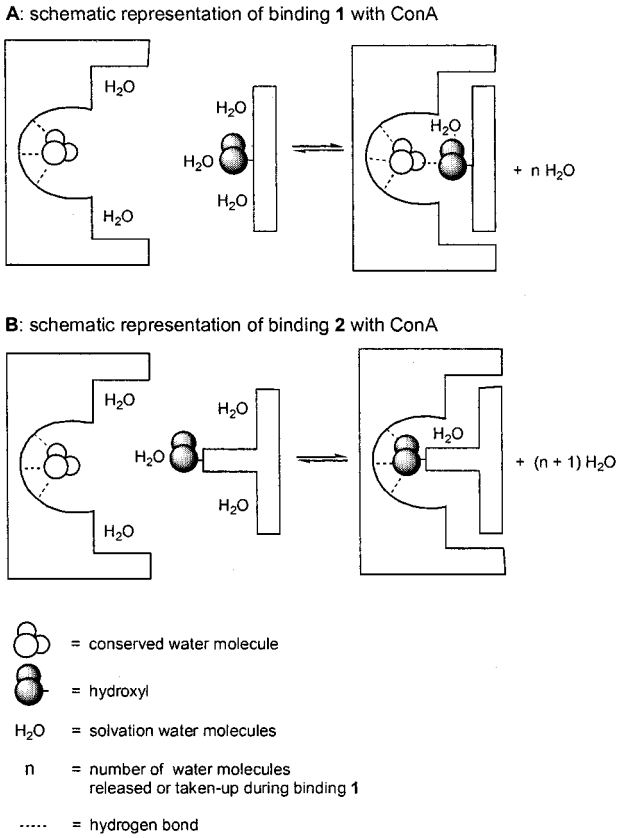

Figure 3. Schematic representation of complexation of Con A with **1** and **2**.

The observed gain in entropy of complexing **2** ($T\Delta\Delta S = 1.1$ kcal mol^{-1} at 298 K), however, is smaller than the expected maximum value. Probably, the entropy of displacement of the highly ordered water molecule to bulk solution is partly offset by the conformational restriction of the hydroxyethyl side chain. Molecular dynamics simulations of **2** in solution and in the complex with Con A showed a significant reduction in flexibility of the hydroxyethyl side chain upon binding, supporting this postulate.

The loss of enthalpy in binding of **2** with Con A was surprising because the structural studies had indicated that its hydroxyethyl moiety could make the same interactions with the protein binding site as made by the conserved water in the complex of **1** with Con A. NMR and MD simulations have also shown that solution conformational properties of the two compounds are very similar.

A possible explanation of the loss of enthalpy came from analyzing differences in hydrogen bonding between the interactions of **1** and **2** with Con A.[52] The change in enthalpy (ΔH) associated with changes in overall hydrogen bonding during ligand binding can be most easily described by considering the reverse process, namely, ligand dissociation.

The dissociation of the protein−ligand **1** complex, as schematically illustrated in Figure 3A, may be described by three nonphysical steps, whereby the hydrogen bonds between the conserved water molecule, protein, and ligand are broken, followed by return of the uncomplexed water molecule to the bulk solution and rehydration of the exposed protein and ligand. In this model, the conserved water molecule is removed in the first step but replaced in the hydration step, thus, overall it is conserved. This approach, which describes accurately the overall

(46) Bourne, Y.; Roussel, A.; Frey, M.; Rouge, P.; Fontecillacamps, J. C.; Cambillau, C. *Proteins* **1990**, *8*, 365−376.
(47) Bourne, Y.; Abergel, C.; Cambillau, C.; Frey, M.; Rouge, P.; Fontecillacamps, J. C. *J. Mol. Biol.* **1990**, *214*, 571−584.
(48) Swaminathan, C. P.; Surolia, N.; Surolia, A. *J. Am. Chem. Soc.* **1998**, *120*, 5153−5159.
(49) Williams, B. A.; Chervenak, M. C.; Toone, E. J. *J. Biol. Chem.* **1992**, *267*, 22 907−22 911.
(50) Mandal, D.; Bhattacharyya, L.; Koenig, S. H.; Brown, I., R. D.; Oscarson, S.; Brewer, C. F. *Biochemistry* **1994**, *33*, 1157−1162.
(51) Deacon, A.; Gleichmann, T.; Kalb (Gilboa), A. J.; Price, H.; Raftery, J.; Bradbrook, G.; Yariv, J.; Helliwell, J. R. *J. Am. Chem. Soc., Faraday Trans.* **1997**, *93*, 4305−4312.
(52) Cooper, A. *Biophys. Chem.* **2000**, *85*, 25−39.

change in hydrogen bonding, will facilitate comparison of the two complexes.

Step A1: Breaking hydrogen bonds between protein, conserved water, and ligand gives ΔH(A1).

Step B1: Return of this liberated water to bulk solution gives ΔH(B1).

Step C1: Rehydration of exposed protein and ligand **1** gives ΔH(C1).

Consequently, the enthalpy of *formation* of the complex of **1** with Con A can be written as (please note change of sign to express complexation)

$$\Delta H(1) = -[\Delta H(\text{A1}) + \Delta H(\text{B1}) + \Delta H(\text{C1})] \quad (1)$$

Similarly dissociation of the ligand **2**−protein complex, as schematically illustrated in Figure 3B, may be considered as follows:

Step A2: Breaking the protein−ligand **2** hydrogen bonds gives ΔH(A2).

Step B2: Rehydration of exposed protein and ligand **2** gives ΔH(B2).

Thus, the enthalpy of *formation* of the complex of **2** with protein can be written as

$$\Delta H(\mathbf{2}) = -[\Delta H(\text{A2}) + \Delta H(\text{B2})] \quad (2)$$

The difference in binding enthalpy between the two interactions is

$$\Delta\Delta H = \Delta H(\mathbf{2}) - \Delta H(\mathbf{1}) = \Delta H(\text{A1}) + \Delta H(\text{B1}) + \Delta H(\text{C1}) - \Delta H(\text{A2}) - \Delta H(\text{B2}) \quad (3)$$

To simplify this relationship, it is reasonable to assume that the enthalpy of hydration of protein and ligand are similar for the two interactions. These assumptions are based on the fact that the same protein surface is hydrated for both interactions. Desolvation enthalpies of compounds **1** and **2** will be discussed below. Thus, the following approximation is made

$$\Delta H(\text{C1}) = \Delta H(\text{B2}) \quad (4)$$

which leads to

$$\Delta\Delta H = \Delta H(\text{A1}) + \Delta H(\text{B1}) - \Delta H(\text{A2}) \quad (5)$$

To quantify the possible effects, the following definitions have been introduced: p = protein (Con A); l(**1**) = ligand **1**; l(**2**) = ligand **2**; w(c) = conserved water molecule; w(d) = dynamic water molecules; $h_{\text{pw(c)}}$ = enthalpy of formation of protein−conserved water hydrogen bonds in complex with **1**; $h_{\text{l(1)w}}$ = enthalpy of formation of a hydrogen bond between ligand **1** and the conserved water molecule; h_{ww} = enthalpy of formation of a water−water hydrogen bond; $h_{\text{pl(2)}}$ = enthalpy of formation of protein−ligand **2** hydrogen bonds.

Further, the hydrogen bonding network involving solvent water, protein, and ligand will generally be dynamic at normal temperatures, and terms need to be defined that describe the partial occupancy of hydration sites: f_{ww} = fractional occupancy of water−water hydrogen bonds in bulk solvent; f_{cw} = fractional occupancy of conserved water in the protein−ligand **1** complex (it is assumed that $f_{\text{cw}} = 1$); f_{dw} = fractional occupancy of dynamic water in the complexes.

The term ΔH(B1) describes the solvation of an isolated water molecule. To quantify this parameter, the premise is made that a water molecule can in principle form four hydrogen bonds with neighboring donor/acceptor groups based on the tetrahedral ice/water lattice.[53] Each of these four bonds is shared between two molecules. Thus, the return of an isolated water molecule to bulk solvent can contribute a maximum of two hydrogen bonds. Due to thermal fluctuations and the nature of the liquid state, not all bonds will be fully occupied at any one time and fractional occupancy of hydrogen bonds has to be introduced (f_{ww}). Thus, solvation of an isolated water molecule can be expressed as

$$\Delta H(\text{B1}) = 2 f_{\text{ww}} h_{\text{ww}} \quad (6)$$

The difference in the terms ΔH(A1) and ΔH(A2) can be considered as the difference in the hydrogen bond network of the C2 hydroxyl of **1**−water−protein arrangement (Figure 3A) and the direct interaction between the hydroxyethyl moiety **2** with the protein (Figure 3B). All other interactions in the two complexes are very similar and therefore these do not need consideration. The term ΔH(A**1**) can be dissected into enthalpy of formation of protein−water hydrogen bonds [$h_{\text{pw(c)}}$] in the protein cavity and enthalpy of formation of a ligand−water hydrogen bond [$h_{\text{l(1)w(c)}}$]. In addition, X-ray crystal structures of the trimannoside−Con A complex showed that the C2 hydroxyl makes an additional hydrogen bond with a dynamic water molecule [$f_{\text{dw}} h_{\text{l(1)w(d)}}$].[24,25] Therefore, the following expression for ΔH(A1) can be written

$$\Delta H(\text{A1}) = -h_{\text{pw(c)}} - h_{\text{l(1)w(c)}} - f_{\text{dw}} h_{\text{l(1)w(d)}} \quad (7)$$

The term ΔH(A2) is composed of the enthalpy of formation of hydrogen bonds of the side chain hydroxyl of ligand **2** with the protein [$h_{\text{pl(2)}}$]. The computer modeling simulations have indicated that the interactions of this hydroxyl with ASN-14, ASP-16, and ARG-228 of the protein binding site (Figure 1) are very similar to the interactions of the water molecule in the complex with **1** with the same residues. This indicates that

$$\Delta H(\text{A2}) = -h_{\text{pl(2)}} = -h_{\text{pw(c)}} \quad (8)$$

Therefore, it is possible to arrive at an equation that describes the differences in enthalpic contributions for the binding of **1** and **2** (substituting eqs 6, 7, and 8 into 5):

$$\Delta\Delta H = -h_{\text{l(1)w(c)}} - f_{\text{dw}} h_{\text{l(1)w(d)}} + 2 f_{\text{ww}} h_{\text{ww}} \quad (9)$$

Equation 9 shows the balance of energies between the interaction of **1** and **2** with Con A. The water-mediated interaction has as an advantage that additional hydrogen bonds can be formed. In the complex with **1**, the conserved water molecule makes four hydrogen bonds; whereas, in the complex with **2**, the equivalent hydroxyethyl side chain makes only three hydrogen bonds. In the latter case, the hydrogen bond between the C2 hydroxyl of **1** and the conserved water molecule is not present because it is replaced by a covalent bond in the hydroxyethyl side chain. The MD simulation and the X-ray crystal structures of the trimannoside with Con A have shown that this is a short hydrogen bond with very high occupancy. In addition, ITC studies of a 2-deoxytrimannoside with Con A also support the importance of this hydrogen bond. This compound, which was extensively studied by Brewer and coworkers,[54] has a lower affinity for Con A compared to binding of **1**, and the loss of affinity was mainly due to a less favorable

(53) Eisenberg, D.; Kauzman, W. *The Structure and Properties of Water*; Oxford University Press: Oxford, 1969.

(54) Gupta, D.; Dam, T. K.; Oscarson, S.; Brewer, F. C. *J. Biol. Chem.* **1997**, *272*, 6388−6392.

enthalpy of binding ($\Delta\Delta H$ = 1.1 kcal mol^{-1} at 298 K). In addition, the C2 hydroxyl of **1** can make further hydrogen bonds (a maximum of three), and the X-ray crystal structure of Con A with a trimannoside showed that this hydroxyl makes at least one additional hydrogen bond with another water molecule. Thus, the abolition of the C2 hydroxyl group of **2** results in the loss of at least two hydrogen bonds. On the other hand, the direct interaction of ligand **2** with Con A results in return of a water molecule to the bulk solution, which provides a favorable enthalpy of $2f_{ww}h_{ww}$.

To proceed numerically, it is assumed that with the exception of the conserved water molecule in Figure 3A, the fractional occupancies of the dynamic water molecule in the binding site and bulk water have a similar *f*-value ($f_{ww} = f_{dw} = f$). Furthermore, the simplification is made that all hydroxyl−hydroxyl hydrogen bonds have approximately the same enthalpy of formation (h) with typical values in the range −4 to −6 kcal mol^{-1}.[53,55,56] Therefore, eq 9 simplifies to

$$\Delta\Delta H = -h(1 - f) \tag{10}$$

The fractional occupancy of water hydrogen bonds in the bulk water is likely to be of the order of 70% at physiological temperatures.[53,55,56] Consequently, a difference in binding enthalpy of 1.2−1.8 kcal mol^{-1} between compounds **1** and **2** is to be expected, which compares favorably with the experimentally determined value (2.3 kcal mol^{-1}). Thus, this analysis indicates that an indirect protein−ligand interaction, mediated by a conserved water molecule, may enthalpically be more favorable due to a large number of hydrogen bonds in the complex that have higher occupancies.

To put the current results in context, it is useful to note that previous studies have also shown that water molecules in carbohydrate−protein complexes may stabilize interactions. For example, the affinity of arabinose binding protein (ABP) for L-arabinose (Ara) is 2.5 times higher than that for D-galactose (Gal).[57−60] The replacement of Gal with Ara results in the inclusion of one water molecule in the position initially occupied by the CH_2OH group of Gal. This substitution allows the formation of one additional hydrogen bond in the ABP−Ara complex, which was used to explain the higher affinity. Our analysis, however, shows that the enthalpy penalty for incorporation of a water molecule in a protein−ligand structure is larger than one hydrogen bond (approximately 1.5 H-bonds). Connelly et al.[61] found that the desolvation of uncharged polar groups of proteins can be a highly unfavorable process at 298 K. They changed tyrosine to phenylalanine in FK506 binding protein, abolishing a hydrogen bond in the protein−ligand (rapamycin) complex. Surprisingly, the mutated protein had a more favorable enthalpy of binding for the rapamycin ligand. High resolution X-ray crystallography revealed that two water molecules bound to the tyrosine hydroxyl of the natural protein. Thus, they showed that removal of the two water molecules upon complex formation is, enthalpically, an unfavorable process. The less favorable enthalpy of binding of the native protein was compensated for, in part, by a more favorable entropy term. This entropy term was probably due to return of bound water to the bulk solvent.

Several assumptions and simplifications have been made that require further discussion. Other studies from our laboratory have indicated that hydrogen bonds between a saccharide and water are stronger than water−water hydrogen bonds,[62] and this factor would further favor binding of **1**. In the proposed model, the assumption is made that the desolvation enthalpies for the two compounds are similar (eq 4). Compound **2** requires, however, additional desolvation of the ethyl moiety, which may cause an energetic effect. Model studies with simple organic molecules have indicated that in aqueous media, burial of aliphatic groups is enthalpically unfavorable. This effect probably originates from removal of ordered water molecules in the first hydration shell of a hydrophilic solute.[63] Recently, Toone and co-workers showed,[64] however, that the enthalpy of desolvation is more complex and depends on the arrangement of polar and apolar atoms and not simply on the number and type. Their findings were in agreement with Lemieux's hydrophobic effect,[16] which predicts that water molecules at polyamphiphilic surfaces are more disordered. Removal of this water is predicted to cause a *favorable* enthalpy of binding. It is to be expected that the incorporation of the ethyl moiety in ligand **2** increases its polyamphiphilic nature and consequently desolvation of this moiety may contribute favorably to the enthalpy of binding. The interaction of the protein with the ethyl moiety was also investigated and no unfavorable contacts were identified. Furthermore, the ethyl moiety makes a similar number of van der Waals contacts with the protein surface as the water molecule. Thus, based on these arguments, the incorporation of the ethyl moiety cannot explain the loss of enthalpy of binding of ligand **2**.

In the model, the temperature dependence of binding enthalpies ($\Delta C_p = \partial\Delta H/\partial T$) arises from the decrease in fractional occupancies, *f*, with increase in temperature. Consequently,

$$\Delta\Delta C_p \approx h(\partial f/\partial T) \tag{11}$$

Numerical estimates based on the heat capacity of bulk water[52] suggest that $h(\partial f/\partial T) \approx 18$ cal K^{-1} mol^{-1}. This number compares favorably with the experimentally determined $\Delta\Delta C_p$ (17 cal K^{-1} mol^{-1}) and strongly indicates that the complex with ligand **1** involves the sequestering of an additional water molecule. Other studies have also indicated that a more negative heat capacity can be attributed to the sequestering of water molecules.[65−68]

Conclusions

The interactions of trimannosides **1** and **2** with Con A were studied to reveal the effects of displacement of well-ordered water molecules on the thermodynamic parameters of protein−ligand complexation. Trisaccharide **2** is derived from **1**, but has

(55) Halkier, A.; Koch, H.; Jorgensen, P.; Christiansen, O.; Nielsen, I. M. B.; Helgaker, T. *Theor. Chem. Acc.* **1997**, *97*, 150−157.
(56) Rose, G. D.; Wolfenden, R. *Annu. Rev. Biophys. Biomol. Struct.* **1993**, *22*, 381−415.
(57) Quiocho, F. A.; Vyas, N. K. Atomic interactions between proteins/enzymes and carbohydrates. In *Bioorganic Chemistry: Carbohydrates*; Hecht, S. M., Ed.; Oxford University Press: New York, 1999; pp 441−597.
(58) Quiocho, F. A. *Nature* **1984,** *310*, 381−386.
(59) Quiocho, F. A. *Biochem. Soc. Trans.* **1993**, *21*, 442−448.
(60) Quiocho, F. A. *Pure Appl. Chem.* **1989**, *61*, 1293−1306.
(61) Connelly, P. R.; Aldape, R. A.; Bruzzese, F. J.; Chambers, S. P.; Fitzgibbon, M. J.; Fleming, M. A.; Itoh, S.; Livingston, D. J.; Navia, M. A.; Thomson, J. A.; Wilson, K. P. *Proc. Natl. Acad. Sci. U.S.A.* **1994**, *91*, 1964−1968.
(62) Kirschner, K. N.; Woods, R. J. *J. Phys. Chem.* **2001**, *105*, 4150−4155.
(63) Muller, N. *Acc. Chem. Res.* **1990,** *23*, 23−28.
(64) Isbister, B. D.; St. Hilaire, P. M.; Toone, E. J. *J. Am. Chem. Soc.* **1995**, *117*, 12 877−12 878.
(65) Ladbury, J. E.; Wright, J. G.; Sturtevant, J. M.; Sigler, P. B. **1994**, *238*, 669−681.
(66) Guinto, E. R.; Cera, E. D. *Biochemistry* **1996**, *35*, 8800−8804.
(67) Schwaz, F. P.; Tello, D.; Goldbaum, F. A.; Mariuzza, F. A.; Poljak, R. J. *Eur. J. Biochem* **1995**, *228*, 388−394.
(68) Morton, C. J.; Ladbury, E. J. *Protein Sci.* **1996**, *5*, 2115−2118.

the hydroxyl at C2 of the central mannose unit replaced by a hydroxyethyl moiety. Upon binding, this artificial moiety displaces a conserved water molecule present in the Con A binding site. As expected, the ITC measurements showed that **2** has a more favorable entropy of binding compared to **1**. This term likely arises from return of the highly ordered water molecule to bulk solution. The order of magnitude of the entropy gain is in agreement with values predicted by Dunitz.[22] The favorable entropic term was offset by a relatively large unfavorable enthalpy term. Structural studies by NMR spectroscopy and MD simulations indicate that the hydroxyethyl side chain of **2** can establish the same hydrogen bonds in a low-energy conformation with the protein binding site as mediated by the water molecule in the complex of **1** with Con A. In addition, hydrogen bonds in the simulated complexes of **1** and **2** with Con A are very similar to those observed in X-ray crystal structures of Con A with a trimannoside. Thus, there is no loss of interaction with the protein binding site or change in conformational properties that can explain the loss of enthalpy of binding. Analyzing the hydrogen bonding interactions indicates that in both complexes the same number of hydrogen bonds were formed. However, the indirect interaction mediated by the conserved water molecule may enthalpically be more favorable due to a large number of hydrogen bonds in the complex that have higher occupancies than in bulk solvent.

Materials and Methods

Nomenclature. The relative orientation of glycosidic linkages is described by a set of torsional angles: ϕ_{1-3} = H1′−C1′−O1′−C3 and ψ_{1-3} = C1′−O1′−C3−H3 for the Manα(1→3)Man linkage and ϕ_{1-6} = H1″−C1″−O1″−C6, ψ_{1-6} = C1″−O1″−C6−C5, and ω_{1-6} = O1″−C6−C5−O5 for the Manα(1→6)Man linkage. The side-chain dihedral angles are defined by χ_1 = C1−C2−C2‴−C1‴ and χ_2 = C2−C2‴−C1‴−O1‴.

NMR Spectroscopy. All data were collected on Varian Inova spectrometers at 500 or 600 MHz. The ^{1}H and ^{13}C spectra of modified trisaccharides **1** and **2** were completely assigned by a combination of COSY, TOCSY, and HSQC experiments. Vicinal coupling constants between H5 and H6 protons were measured directly from the H6 signals in the 1D spectra and were used to determine the rotamer populations of the ω dihedral angle of the α(1→6) linkage. The values of $^3J_{H5,H6R}$ and $^3J_{H5,H6S}$ are related via a Karplus-type relationship to the dihedral angle around the bond that connects the coupled atoms.[31] Heteronuclear trans-glycosidic coupling constants are sensitive to the orientation around glycosidic linkages and were used to determine the glycosidic torsion angles of the α(1→3) and α(1→6) linkages.[33] Trans-glycosidic proton−carbon vicinal coupling constants were measured at 500 MHz by using a quantitative HMBC experiment. Two data matrixes, a full HMBC and a reference HMQC of 1024 × 256 complex points, were collected, with a proton spectral width of 3100 Hz and a carbon spectral width of 9055 Hz. Data were processed with Felix software in a standard way (Gaussian line broadening, zero-filling in both dimensions) without any t1-noise minimization. The coupling constants extracted from the ratios of peak volumes of the three-bond cross peaks corresponded to the appropriate single bond reference cross peaks. No fitting algorithms were used, as by Zhu et al. no estimation of errors are reported. However, it is expected that the resulting values have errors at least as great as those reported by Zhu et al.[69]

NOE spectra of trisaccharides **1** and **2** in D_2O were measured at mixing times of 50, 100, 250, 500, 750, 1000, 1500, 2000, and 3000 ms with a 1D GOESY experiment[70] and were used to determine interproton distances. Internuclear distances were calculated from the NOE intensities in the linear region of the NOE buildup curves, where an isolated spin-pair approximation is valid, using the intraring H1−H2 NOE as an internal reference.[27,28]

Molecular Dynamics Simulations. All MD simulations were performed under periodic boundary conditions using the SANDER module of AMBER 5.0[71] and employing the all-atom GLYCAM parameter set for oligosaccharides and glycoproteins,[72] on SGI Origin 200, 2000, or Indigo^2 computers. The initial oligosaccharide conformation was set to that observed in the Con A−trimannoside crystal structure (PDB id 1cvn). The atomic charges of the central side-chain-containing residue of **2** were generated by using GAUSSIAN94 at the Hf/6-31G* level with fitting to electrostatic potentials achieved using CHELPG, in a manner analogous to that used in the GLYCAM database.

For solvated simulations, the oligosaccharides were placed in a theoretical box of TIP3P water molecules.[73] The initial solvent configurations were subjected to 10 000 cycles of energy minimization: 9000 steepest descent followed by 1000 conjugate gradient. All minimizations and subsequent dynamics were performed with a dielectric constant of unity and a cutoff value for nonbonded interactions of 8.0 Å. All 1−4 electrostatic and van der Waals interactions were scaled by the standard values (SCEE = 1.2, SCNB = 2.0). Unfavorable contacts were removed by simulated annealing of the solvent: the temperature was raised to 300 K over 20 ps, maintained at 300 K for 60 ps, and then lowered back to 5 K over a further 20 ps. Finally, the energy of the solvent and solute was reminimized by the protocol described above. Newton's equations of motion were integrated by using a 2-fs time-step. Initial atomic velocities were assigned from a Maxwellian distribution at 5 K. During the simulations, a constant temperature of 300 K was maintained through weak coupling to an external bath with a coupling constant of 0.25 ps^{-1}. Bond lengths involving hydrogen were constrained to their equilibrium values using the SHAKE algorithm.[74]

Molecular Modeling of the Complexes between Con A and 1 and 2. Simulations of the ligand−Con A complex were carried out by using a single subunit from the 1cvn X-ray crystal structure. Compound **1** was overlaid in the position of 3,6-di-*O*-(α-D-Man)-α-D-Man in the binding site, and the crystallographic water molecules within 15 Å of the binding site were retained. Protonation of the crystallographic water molecules was achieved by using the GWH module of AMBER, which orients the protons to maximize favorable electrostatic interactions. For the Con A−trisaccharide **2** complex, the side chain was overlaid in the position of the bound water molecule that was present at the C2 position of the central mannose residue. A spherical cap of waters of 23 Å radius was placed over the binding site, which was restrained with a half-harmonic potential. Energy minimization and simulated annealing were performed as discussed above. The positions of atoms of the protein outside the defined 15 Å active site region were held rigid by using the belly option of SANDER.

Microcalorimetry. The saccharides **1** and **2** were obtained by organic synthesis and details will be reported elsewhere. Isothermal titration calorimetry (ITC) experiments to measure the binding of the saccharides to Con A were performed over a 10−37 °C (283−310 K) temperature range using Microcal MCS and VP−ITC titration microcalorimeters following standard procedures[75,76] with a 250-μL injection syringe. Con A (Sigma) was used without further purification and was dissolved in buffer (0.1 M Tris, 0.5M NaCl, 1mM $MnCl_2$, 1 mM $CaCl_2$,

(69) Zhu, G.; Renwick, A.; Bax, A. *J. Magn. Reson. A.* **1994**, *110*, 257−261.

(70) Stonehouse, J.; Adell, P.; Keeler, J.; Shaka, A. J. *J. Am. Chem. Soc.* **1994**, *116*, 6037−6038.

(71) Case, D. A.; Pearlman, D. A.; Caldwell, J. W.; Cheatham, T. E., III; Ross, W. S.; Simmerling, C. L.; Darden, T. A.; Merz, K. M.; Stanton, R. V.; Cheng, A. L.; Vincent, J. J.; Crowley, M.; Ferguson, D. M.; Radmer, R. J.; Seibel, G. L.; Singh, U. C.; Weiner, P. K.; Kollman, P. A. *AMBER 5.0*, 5.0 ed.; University of California: San Francisco.

(72) Woods, R. J.; Dwek, R. A.; Edge, C. J. *J. Phys. Chem.* **1995**, *99*, 3832−3846.

(73) Jorgensen, W. L.; Chandrasekhar, J.; Madura, J. D.; Impey, R. W.; Klein, M. L. *J. Phys. Chem.* **1983**, *79*, 926−935.

(74) Ryckaert, J.-P.; Ciccotti, G.; Berendsen, H. J. *J. Comput. Phys.* **1977**, *23*, 327−341.

(75) Wiseman, T.; Williston, S.; Brandts, J. F.; Lin, L. N. *Anal. Biochem.* **1989**, *179*, 131−137.

(76) Cooper, A.; Johnson, C. M. In *Methods in Molecular Biology. Microscopy, Optical Spectroscopy, and Macroscopic Techniques*; Jones, C., Mulloy, B., Thomas, B., Eds.; Humana Press: Totowa, NJ, 1994; pp 137−150.

pH 7.0) and degassed gently immediately before use. Saccharide ligands were dissolved in the same buffer. Protein concentrations in the ITC cell were determined from UV absorbance measurements at 280 nm using molar extinction coefficients: $\epsilon_{280} = 33\,000$ (Con A). A typical binding experiment involved a 1-μL preinjection followed by 25 10-μL injections of ligand solution (typically 5−10 mM concentration) into the ITC cell (ca. 1.4 mL active volume) containing protein at concentrations ($c = 0.1-0.5$ mM) chosen to ensure that $Kc > 1$ for optimal data analysis. Control experiments were performed under identical conditions by injection of ligand into buffer alone (to correct for heats of ligand dilution) and injection of buffer into the protein mix (to correct for heats of dilution of the protein). Similar ITC experiments with the monosaccharide ligand, methyl α-D-mannopyranoside (Sigma), were done in parallel to compare with previous determinations. Integrated heat effects, after correction for heats of dilution, were analyzed by nonlinear regression in terms of a simple single-site binding model using the standard Microcal ORIGIN software package. For each thermal titration curve this yields estimates of the apparent number of binding sites (N) on the protein, the binding constant (K/M^{-1}), and the enthalpy of binding (ΔH/kcal mol^{-1}). In cases of weak ligand binding (monosaccharide), the titration curve is too gradual to allow unambiguous estimation of N, and in such cases the stoichiometry was fixed at $N = 1$ for regression fits. ΔC_p was obtained from weighted linear regression of ΔH versus temperature data, with standard errors estimated from multiple determinations. Other thermodynamic quantities were calculated by using standard expressions (eq 12):

$$\Delta G = -RT \ln K = \Delta H - T\Delta S \tag{12}$$

JA004315Q